

Supporting Information

[Au₁₄(2-SAdm)₉(Dppe)₂]⁺: a gold nanocluster with crystallization-induced emission enhancement phenomenon

Dong Liu,[‡] Guiqi Gao,[‡] Yongyu Zhang, Qinzhen Li, Sha Yang, Jinsong Chai,* Haizhu Yu* and Manzhou Zhu*

Department of Chemistry and Centre for Atomic Engineering of Advanced Materials, Key Laboratory of Structure and Functional Regulation of Hybrid Materials of Ministry of Education, Institutes of Physical Science and Information Technology and Anhui Province Key, Laboratory of Chemistry for Inorganic/Organic Hybrid Functionalized Materials, Anhui University, Hefei, 230601, China

*E-mails of corresponding authors: chajjs@ahu.edu.cn; yuhaizhu@ahu.edu.cn; zmz@ahu.edu.cn

[‡] These authors contributed equally to this work

1. Chemicals

All solvents and reagents used in this study were commercially available and were used without further purification. Dichloromethane (DCM, HPLC grade), methanol (MeOH, HPLC grade), toluene (HPLC grade), n-hexane (n-Hex, HPLC grade), acetonitrile (MeCN, HPLC grade), ethanol (EtOH, HPLC grade), 2-adamantanethiol (2-HSAdm, $\geq 98\%$), D-penicillamine (DPA, $\geq 98\%$), (E)-1,2-bis(diphenylphosphine)ethylene (Dppe, $\geq 98\%$), sodium hexafluoroantimonate (NaSbF_6 , $\geq 98\%$), potassium hexafluorophosphate (KPF_6 , $\geq 99\%$), sodium molybdenum oxide (Na_2MoO_4 , $\geq 99\%$), sodium tetraphenylboron (NaBPh_4 , $\geq 99.5\%$), sodium *p*-toluenesulfonate (NaTsO , $\geq 98\%$), $\text{HAuCl}_4 \cdot 4\text{H}_2\text{O}$ ($\geq 99.99\%$, based on metal), NaOH ($\geq 99.9\%$) and sodium borohydride (NaBH_4 , $\geq 98\%$), Potassium chloride (KCl , $\geq 99.5\%$), sodium chloride (NaCl , $\geq 99.5\%$), aluminum chloride (AlCl_3 , $> 98\%$), ferric chloride (FeCl_3 , $\geq 99\%$), copper chloride (CuCl_2 , $\geq 98\%$), cadmium chloride (CdCl_2 , $\geq 99\%$), cobalt nitrate ($\text{Co}(\text{NO}_3)_2$, $\geq 99\%$), Nickel chloride (NiCl_2 , $\geq 99\%$), mercury nitrate ($\text{Hg}(\text{NO}_3)_2$, $\geq 98\%$), Silver nitrate (AgNO_3 , $\geq 99\%$), zinc nitrate ($\text{Zn}(\text{NO}_3)_2$, $\geq 99\%$), Chloroform-D (CDCl_3 , $\geq 99.8\%$) were all purchased from Shanghai Aladdin Biochemical Technology Co., LTD. The ultrapure water ($\geq 18.2 \text{ M}\Omega$) used in this study was purified on a Millipore system (Millipore USA). Before use, all glassware should be washed with aqua regia and rinsed with ultrapure water.

2. Synthesis of $[\text{Au}_{14}(\text{2-SAdm})_9(\text{Dppe})_2]\text{X}$ ($\text{X} = \text{SbF}_6^-$, PF_6^- , BPh_4^- , TsO^- , 0.5 MoO_4^{2-})

60 mg of DPA was dissolved in 10 mL of ultrapure water, followed with the addition of 400 μL HAuCl_4 stock solution (0.2 g/mL in water). After the color of the solution changed from light yellow to colorless, 2 mL of NaOH aqueous solution (1 mol/L) was added. Then, 20 mg of NaBH_4 dissolved in 2 mL of water was added. The color of the solution changed into dark brown in 5 min. Then 100 mg of 2-HSAdm and 20 mg of (E)-1,2-bis(diphenylphosphine)ethylene dissolved in 10 mL of DCM was added into the reaction. The mixed solution was stirred violently to proceed the two-phase ligand exchange process. After about 2 h, the DCM phase was collected and centrifuged at 10000 rpm for 2 min. The supernatant is concentrated by rotary evaporation and then washed with methanol to remove excess ligands. After redissolved in DCM, the raw product containing Au_{14} was purified on thin layer chromatography (TLC) plate ($\text{MeCN}/\text{DCM} = 1:1$). The as-purified Au_{14} was dissolved in MeOH and then different types of counterions (SbF_6^- , PF_6^- , BPh_4^- , TsO^- , MoO_4^{2-}) were added. The precipitate was then collected by centrifugation. Pure Au_{14} was crystallized in DCM/n-Hex to obtain high-quality single crystals.

3. Au_{14} in amorphous state for fluorescence test

Au_{14} in amorphous state was obtained by mixing DCM solution of Au_{14} and n-Hex quickly. The as-obtained powdery precipitate was then dried at room temperature to remove the residual solvent.

4 DOSY ^1H NMR

At room temperature, 50 mg of Au₁₄ crystals were dissolved in 600 μL of deuteriochloroform solution as the initial concentration, and then another 400 μL of deuteriochloroform was added each time for dilution and 600 μL was taken to obtain a series of test solutions with different concentrations.

5. Computational Details

All the structures discussed in this work were calculated at the BP/DND level¹⁻² with the effective core potential (ECP) Pseudopotential³⁻⁴ performed in the DMol³ package.⁵⁻⁷ The convergence tolerances of energy, force, and displacement for the structure relaxation were 1.0×10^{-6} Ha, 2.0×10^{-4} Ha/Å, and 5.0×10^{-4} Å, respectively. Based on the optimized structures, Kohn–Sham calculation was performed with the B3PW91 level of theory^{1,8} on the Gaussian 09 suite of program.⁹ Gold atoms were treated with the SDD basis set and the related effective core potential (ECP), For the remaining atoms, the 6-31G* basis set was used.¹⁰

6. Measurements

All UV-vis spectra in the study were obtained using an Agilent 8453 instrument. ESI-MS measurement results were recorded using a Waters Xevo G2-XS Q ToF mass spectrometer. The source temperature was maintained at 80 °C and the Au₁₄ solution were directly infused into a chamber at a flow rate of 20 μL/min. Single crystal X-ray diffraction (SCXRD) was performed by using graphite monochrome Cu Kα radiation ($\lambda = 1.54186$ Å) at 120 K in liquid nitrogen flow on Stoe Stadivari diffractometer. Fluorescence spectra were obtained from an F-7000 fluorescence spectrophotometer. The nuclear magnetic experiments are all done on the JNM-ECZ400SMHz nuclear magnetic resonance spectrometer. The EPR was measured by PLS-SXE300+ electron paramagnetic resonance spectromet. X-ray photoelectron spectroscopy (XPS) measurements were performed on an ESCALAB 250Xi XPS spectrometer (Al Kα, $h\nu = 1486.6$ eV) using a monochromatized Al Kα source equipped with an Ar⁺ ion sputtering gun.

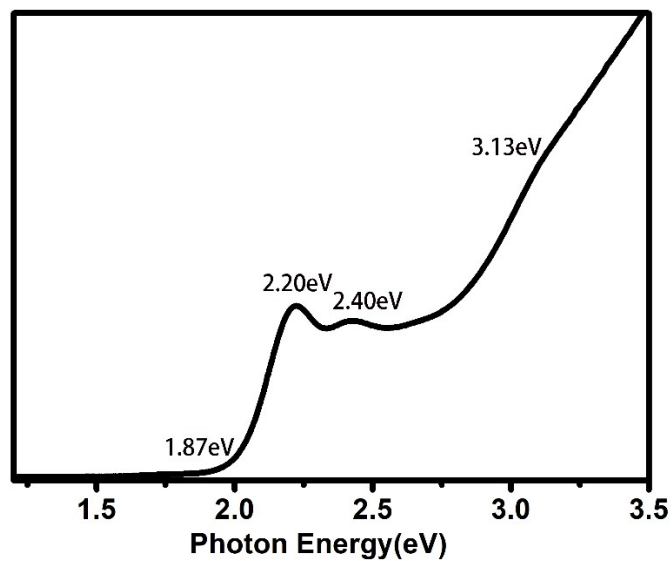


Fig. S1 Photoelectron spectroscopy of Au₁₄.

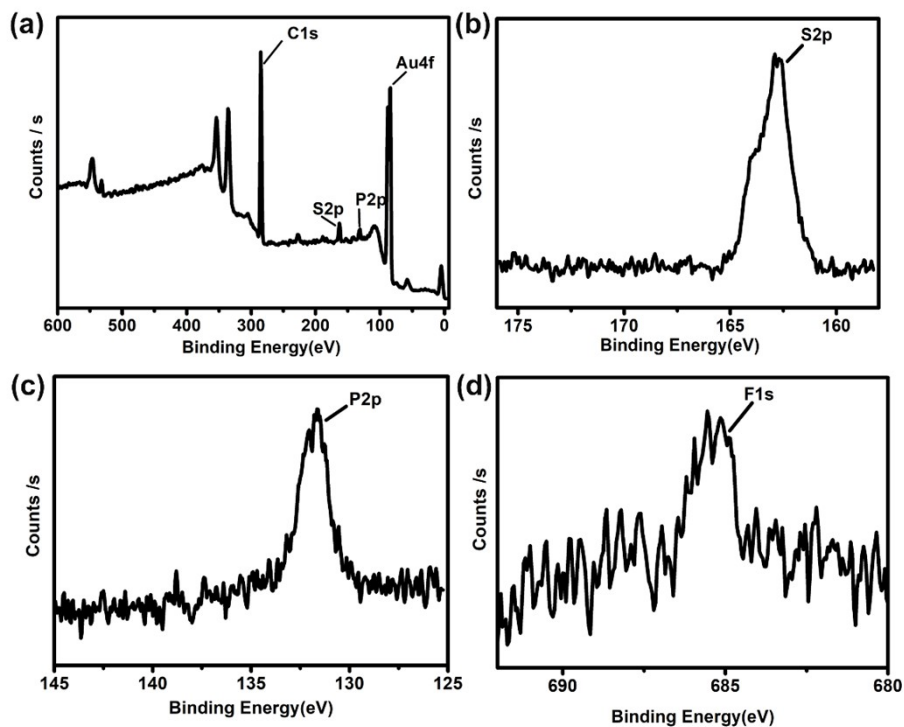


Fig. S2 (a) The survey XPS spectrum, and (b) S 2p, (c) P 2p, (d) F 1s.

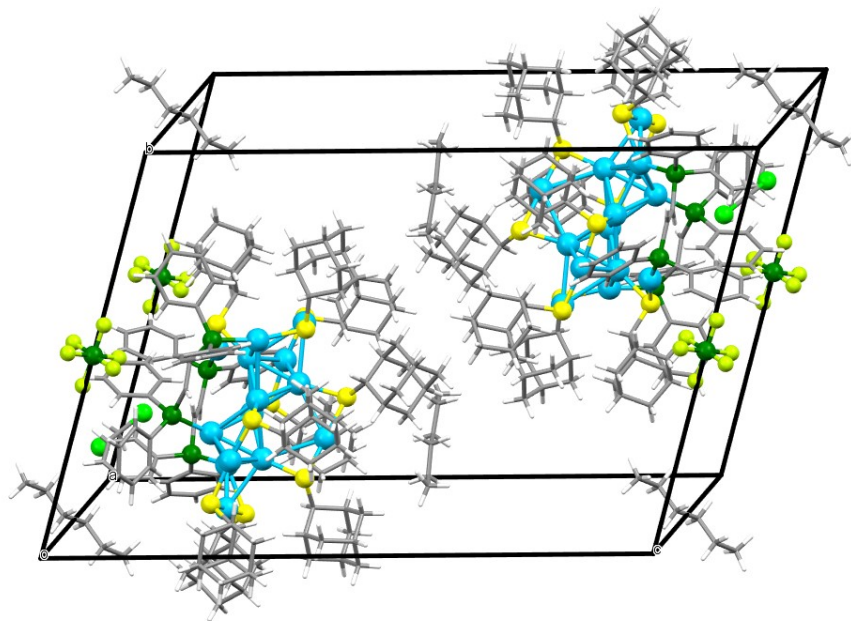


Fig. S3 The unit cell of Au₁₄ nanocluster (labels: Au = blue; S = yellow; P = green; F = lime; Cl = bright green; C = gray; H = white).

Table S1. Crystal data and structure refinement for Au₁₄

CCDC code	2286900
Empirical formula	C _{151.5} H ₂₀₁ Au ₁₄ ClF ₃ P _{4.5} S ₉
Formula weight	5300.00
Temperature/K	120.0
Crystal system	triclinic
Space group	P-1
a/Å	15.8928(3)
b/Å	20.0176(4)
c/Å	29.1486(6)
α/°	75.0450(10)
β/°	78.775(2)
γ/°	78.621(2)
Volume/Å ³	8681.3(3)
Z	2
ρ _{calc} /cm ³	2.028
μ/mm ⁻¹	23.505
F(000)	4943.0
Crystal size/mm ³	0.27 × 0.25 × 0.12
Radiation	Cu Kα (λ = 1.54186)
2θ range for data collection/°	9.258 to 125
Index ranges	-12 ≤ h ≤ 18, -21 ≤ k ≤ 23, -33 ≤ l ≤ 31
Reflections collected	53361
Independent reflections	26608 [R _{int} = 0.0413, R _{sigma} = 0.0477]
Data/restraints/parameters	26608/913/1666
Goodness-of-fit on F ²	1.038
Final R indexes [I ≥ 2σ (I)]	R ₁ = 0.0533, wR ₂ = 0.1406
Final R indexes [all data]	R ₁ = 0.0625, wR ₂ = 0.1552
Largest diff. peak/hole / e Å ⁻³	3.52/-3.70

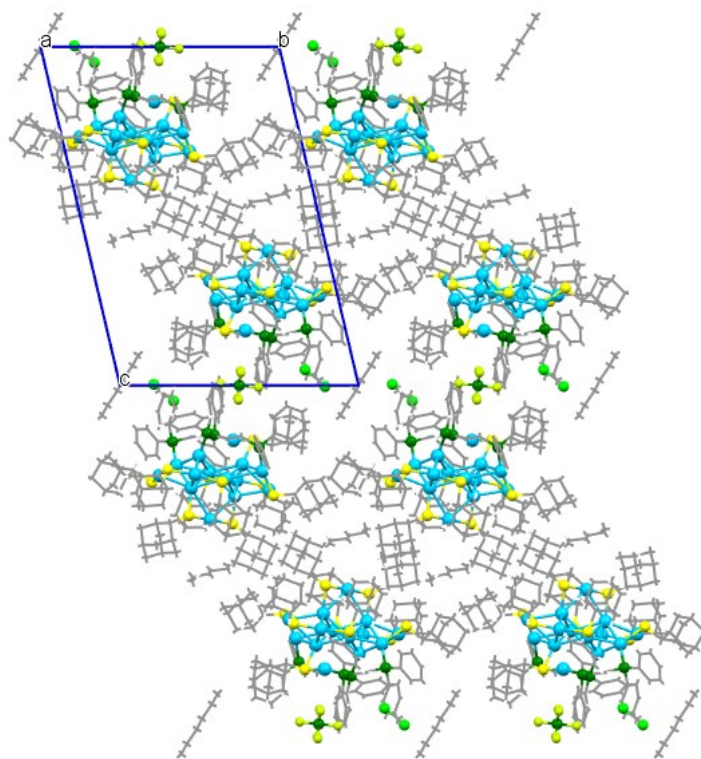


Fig. S4 Packing mode of the Au₁₄ along the a axis (labels: Au = blue; S = yellow; P = green; F = lime; Cl = bright green; C = gray).

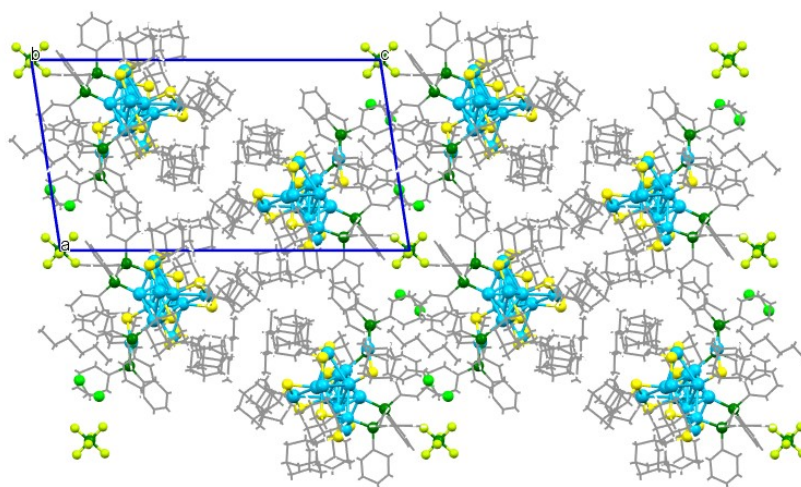


Fig. S5 Packing mode of the Au₁₄ along the b axis (labels: Au = blue; S = yellow; P = green; F = lime; Cl = bright green; C = gray).

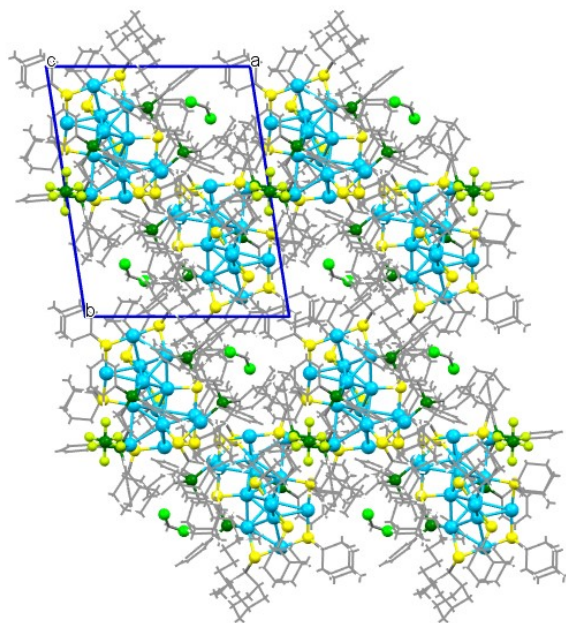


Fig. S6 Packing mode of the Au_{14} along the c axis (labels: Au = blue; S = yellow; P = green; F = lime; Cl = bright green; C = gray).

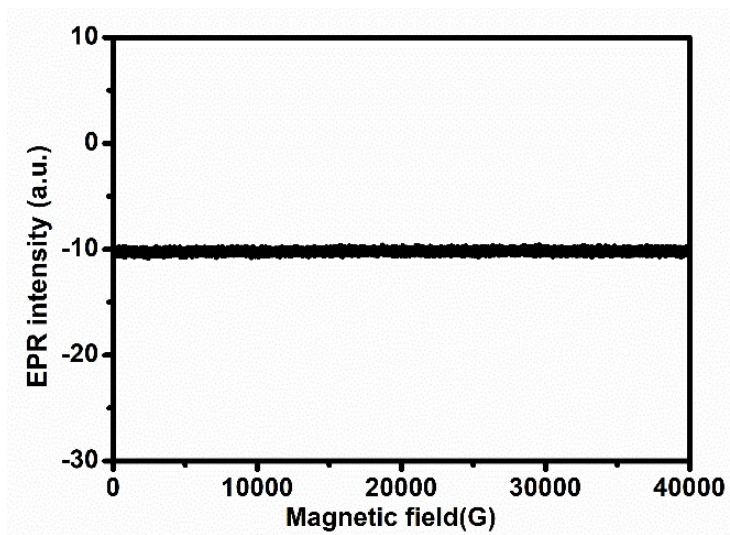


Fig. S7 EPR signal diagram of Au_{14} nanocluster

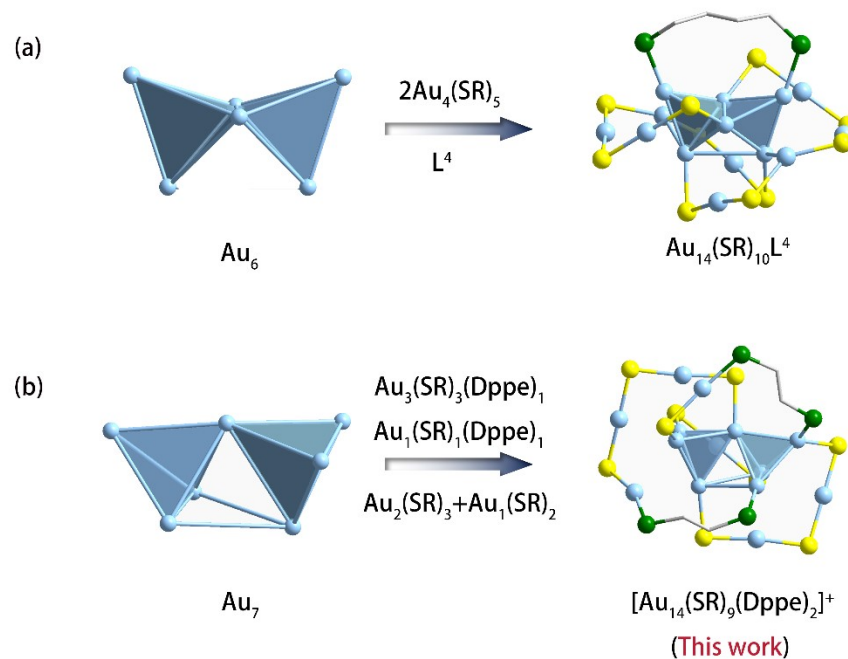


Fig. S8 Comparison of the crystal structure between two different Au_{14} nanoclusters. (Label: Au = blue-gray; S = yellow; P = green; C = gray)

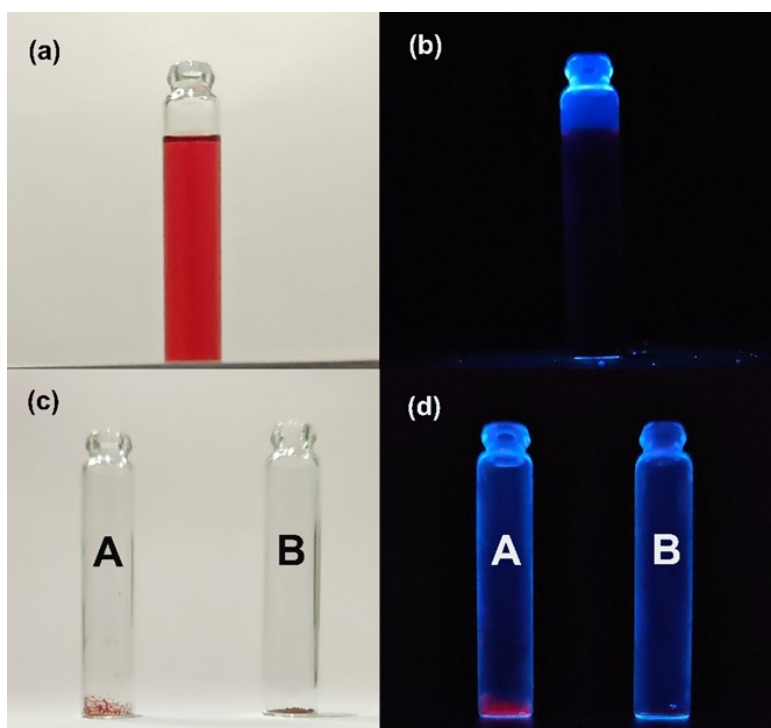


Fig. S9 Fluorescence photographs of Au_{14} in different states. (a) In a liquid state; (b) Exposure under dark conditions; (c) in the crystal state (A) and amorphous state (B); (d) fluorescent photographs of crystals and amorphous under 365-nm illumination.

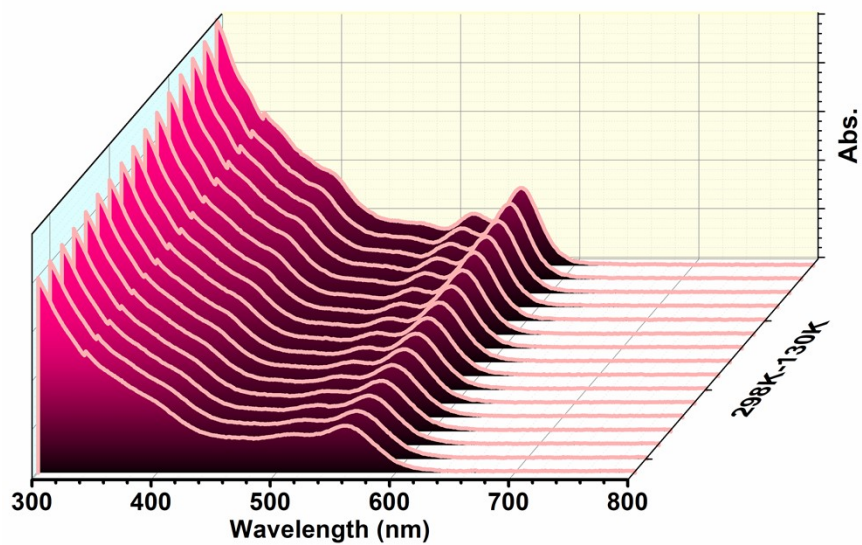


Fig. S10 UV-vis spectra of Au₁₄ nanoclusters with the temperature from 298 K to 130 K.

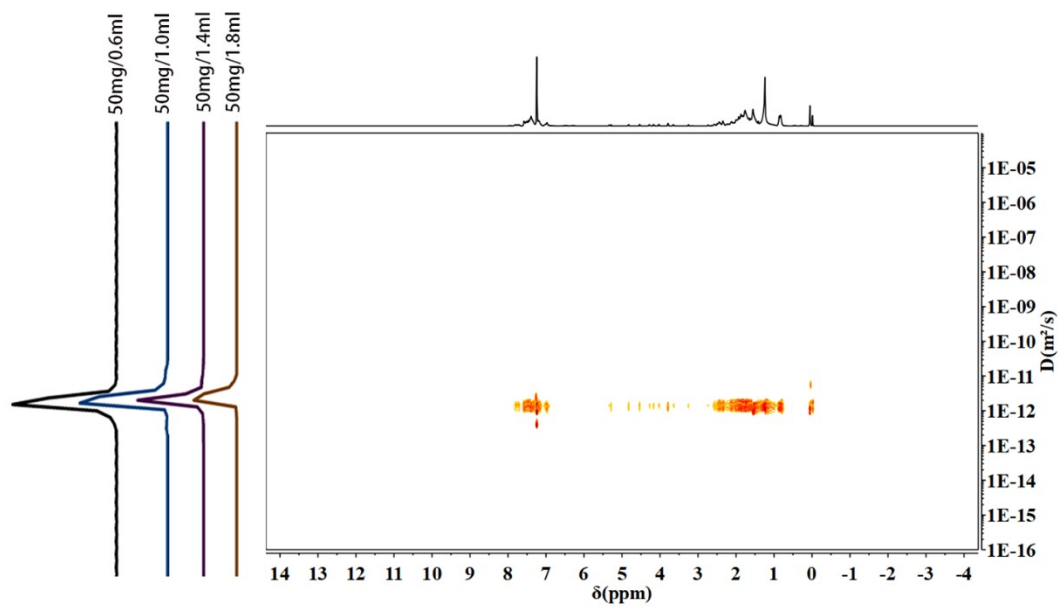


Fig. S11 DOSY ¹H NMR spectra of Au₁₄ with different concentration (solvent: CDCl₃).

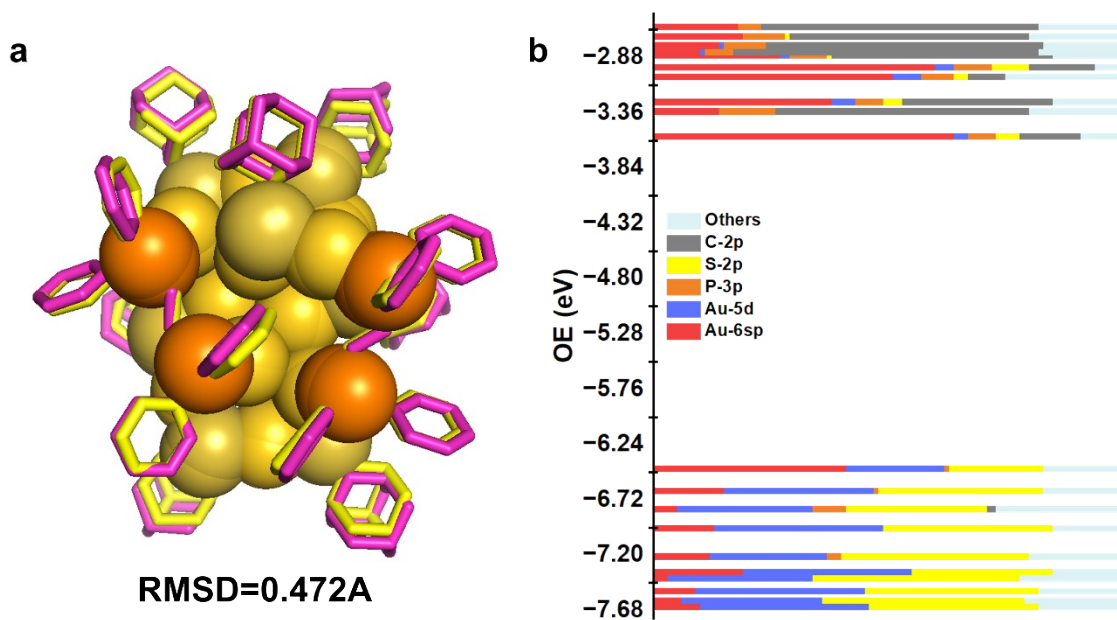


Fig. S12 Electron state analysis of Au₁₄ nanoclusters

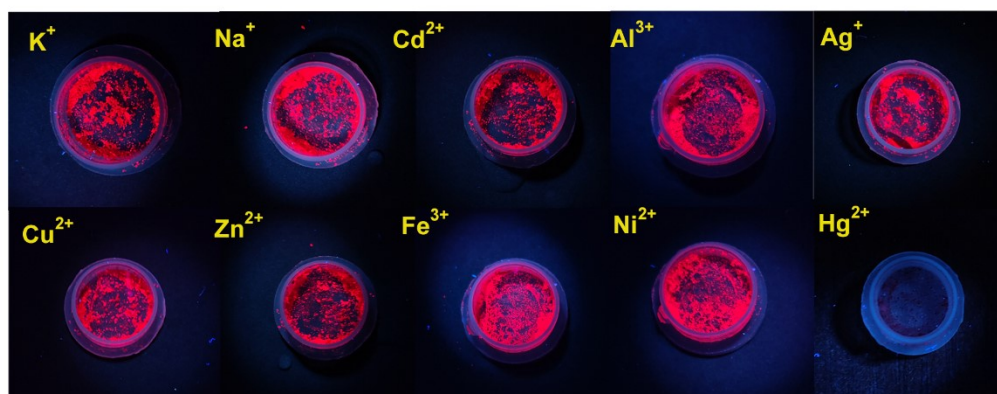


Fig. S13 Photograph of the Au₁₄ crystals under 365-nm illumination with the addition of different ions (K⁺, Na⁺, Ag⁺, Cu²⁺, Hg²⁺, Cd²⁺, Zn²⁺, Ni²⁺, Al³⁺, Fe³⁺; 3 mmol/L in water).

Table S2. Quantum yield comparison of gold nanoclusters

Nanocluster	QY (%) ^[a]	Ref.
[Au ₂₅ (C ₂ H ₄ Ph) ₁₈] ⁻	0.01	11
Au ₆₀ S ₈ (SCH ₂ Ph) ₃₆ (Au ₆₀ S _{8r})	9	12
Au ₆₀ S ₈ (SCH ₂ Ph) ₃₆ (Au ₆₀ S _{8n})	5.6	12
[Au ₈ (dppm) ₄ S ₂]Cl ₂	4.57	13
Au ₂₈ (TBBT) ₂₀	1.6	14
Au ₂₈ (S- <i>c</i> -C ₆ H ₁₁) ₂₀	0.1	14
[Au ₁₈ (S- <i>c</i> -C ₆ H ₁₁) ₁₄]	0.1	15

Au₄₂(PET)₃₂	11.9	16
Au₃₈S₂(S-Adm)₂₀	15	17
Au₂₁(S-Adm)₁₅	4	17
Au₂₃(S-<i>c</i>-C₆H₁₁)₁₆	0.4	18
Au₂₅(PET)₅(PPh₃)₁₀X₂	8	19
Au₂₄(PET)₅(PPh₃)₁₀X	1	19
Au₂₈(SCH₂Ph-<i>t</i>Bu)₂₂	5.1	20
Au₂₄(SCH₂Ph-<i>t</i>Bu)₂₀	3	21
[Au₁₃(Dppe)₅Cl₂]³⁺	0.71	22
Au₃₈(PET)₂₆	1.8	23
[Au₁₄(2-SAdm)₉Dppe]⁺	5.05	This work

[a] QY:quantum yield

1. J. P. Perdew and Y. Wang, *Phys. Rev. B.*, 1992, **45**, 13244–13249.
2. A. D. Becke, *J. Chem. Phys.*, 1988, **88**, 2547–2553.
3. M. Dolg, U. Wedig, H. Stoll and H. Preuss, *J. Chem. Phys.*, 1987, **86**, 866–872.
4. A. Bergner, M. Dolg, W. Kuechle, H. Stoll and H. Preuss, *Mol. Phys.*, 1993, **80**, 1431–1441.
5. B. Delley, *J. Chem. Phys.*, 1990, **92**, 508–517.
6. B. Delley, *J. Phys. Chem.*, 1996, **100**, 15, 6107–6110.
7. B. Delley, *J. Chem. Phys.*, 2000, **113**, 7756–7764.
8. A. D. Becke, *J. Chem. Phys.*, 1993, **98**, 5648–5652.
9. Gaussian 09, Revision D.02, M. J. Frisch, G. W. Trucks, H. B. Schlegel, G. E. Scuseria, M. A. Robb, J. R. Cheeseman, G. Scalmani, V. Barone, B. Mennucci, G. A. Petersson, H. Nakatsuji, M. Caricato, X. Li, H. P. Hratchian, A. F. Izmaylov, J. Bloino, G. Zheng, J. L. Sonnenberg, M. Hada, M. Ehara, K. Toyota, R. Fukuda, J. Hasegawa, M. Ishida, T. Nakajima, Y. Honda, O. Kitao, H. Nakai, T. Vreven, Jr., J. A. Montgomery, J. E. Peralta, F. Ogliaro, M. Bearpark, J. J. Heyd, E. Brothers, K. N. Kudin, V. N. Staroverov, R. Kobayashi, J. Normand, K. Raghavachari, A. Rendell, J. C. Burant, S. S. Iyengar, J. Tomasi, M. Cossi, N. Rega, J. M. Millam, M. Knox, J. B. Cross, V. Bakken, C. Adamo, J. Jaramillo, R. Gomperts, R. E. Stratmann, O. Yazyev, A. J. Austin, R. Cammi, C. Pomelli, J. W. Ochterski, R. L. Martin, K. Morokuma, V. G. Zakrzewski, G. A. Voth, P. Salvador, J. J. Dannenberg, S. Dapprich, A. D. Daniels, O. Farkas, J. B. Foresman, J. V. Ortiz, J. Cioslowski, D. J. Fox, Wallingford CT, 2009.
10. V. A. Rassolov, M. A. Ratner, J. A. Pople, P. C. Redfern, and L. A. Curtiss, *J. Comp. Chem.*, 2001, **22**, 976–984.
11. Z. Wu and R. Jin, *Nano Lett.*, 2010, **10**, 2568–2573.
12. Z. Gan, Y. Liu, L. Wang, S. Jiang, N. Xia, Z. Yan, X. Wu, J. Zhang, W. Gu, L. He, J. Dong, X. Ma, J. Kim, Z. Wu, Y. Xu, Y. Li and Z. Wu, *Nat. Commun.*, 2020, **11**, 5572.
13. S. Zhang, L. Feng, R. D. Senanayake, C. M. Aikens, X. Wang, Q. Zhao, C. Tung and D. Sun, *Chem. Sci.*, 2018, **9**, 1251–1258.
14. Y. Chen, M. Zhou, Q. Li, H. Gronlund and R. Jin, *Chem. Sci.*, 2020, **11**, 8176–8183
15. S. Chen, S. Wang, J. Zhong, Y. Song, J. Zhang, H. Sheng, Y. Pei and M. Zhu, *Angew. Chem., Int. Ed.*, 2015, **54**, 3145–3149.

16. L. Luo, Z. Liu, X. Du, and R. Jin, *J. Am. Chem. Soc.*, 2022, **144**, 19243–19247.
17. Q. Li, C. J. Zeman IV, G. C. Schatz, and X. W. Gu, *ACS Nano*, 2021, **15**, 16095–16105.
18. Q. Li, M. Zhou, W. Y. So, J. Huang, M. Li, D. R. Kauffman, M. Cotlet, T. Higaki, L. A. Peteanu, Z. Shao and R. Jin, *J. Am. Chem. Soc.*, 2019, **141**, 5314–5325.
19. Q. Li, C. J. Zeman IV, Z. Ma, G. C. Schatz, X. W. Gu, *Small*, 2021, **17**, 2007992.
20. J. Dong, Z. Gan, W. Gu, Q. You, Y. Zhao, J. Zha, J. Li, H. Deng, N. Yan, Z. Wu, *Angew. Chem., Int. Ed.*, 2021, **60**, 17932–17936.
21. Z. Gan, Y. Lin, L. Luo, G. Han, W. Liu, Z. Liu, C. Yao, L. Weng, L. Liao, J. Chen, X. Liu, Y. Luo, C. Wang, S. Wei, Z. Wu, *Angew. Chem., Int. Ed.*, 2016, **55**, 11567–11571.
22. J. Zhang, Y. Zhou, K. Zheng, H. Abroshan, D. R. Kauffman, J. Sun, and G. Li, *Nano Res.*, 2018, **11**, 5787–5798.
23. L. Luo, Z. Liu, X. Du, and R. Jin, *Commun. Chem.*, 2023, **6**, 22.